Thermal Stresses in Monolithic Catalysts

H. J. Viljoen and N. F. J. van Rensburg
Dept. of Chemical Engineering, University of Nebraska, Lincoln, NE 68588

Monolithic catalysts are widely used for the control of air pollution, particularly by the automotive industry. However, it is not limited to automobile usage. Waste gases from certain industrial processes and emissions that contain ecologically harmful constituents are also treated in monolithic catalysts to lower or eliminate the levels of the hazardous or obnoxious components. Previous modeling studies concentrated on the conversion and overall performance of the catalytic system. No studies have been published on the interaction between chemical reaction and thermal stresses in monolithic catalyst systems. It is a well-known fact that these systems do fail periodically, as is the case for several other catalytic systems. Mechanical failure of catalyst supports in packed bed reactors have been reported (Thiart et al., 1990, 1991, 1993). Catalytic gauzes like *Pt* or *Pt − Rh* used for fast exothermic reactions are prone to metal fatigue, work-hardening and catastrophic failure. Large costs are involved in lost production and catalyst replacement. The monolithic catalyst system is now widely used outside automobile exhaust control and new applications might create conditions which unknowingly exceed present mechanical standards. A more fundamental approach towards the effects of thermal stresses on the structure will help designers to become more aware of the problem and to analyze the problem in a scientific manner.

Typical reactions which are carried out in monolithic catalysts lead to strong axial temperature gradients in the channels. Although the monolith can freely expand in the axial direction, it is contained in the radial and azimuthal directions, causing a distributed compressive load on the channel walls. A failure criterion based on the classical plate theory is derived. The failure criterion depends on the axial temperature profile and physical properties of the system like the channel dimensions and the wall thickness. Interestingly, failure is not influenced by the Young's modulus, but it depends on the Poisson ratio and the thermal expansion coefficient.

Model

In the thermoelastic model of thermal stresses, which is quite appropriate for monolithic catalyst structures, the temperature field is decoupled from the stress fields. Therefore, we will first introduce the model that describes the temperature field. We have decided to use the catalytic oxidation of CO as our chemical system.

Chemical reaction model

Consider a single channel of a monolithic honeycomb converter. The channel has a length L, hydraulic diameter D and wall thickness Δt. The average velocity is U. L and L/U are now introduced as scales for length and time. The following dimensionless temperatures, radiation flux and concentrations are defined: $\theta_m = T_m - T_{fi}/T_{fi}$, $q_R = Q_R/\sigma_B T_{fi}^4$, $c_{mn} = C_{mn}/C_{fni}$, where $m \equiv f$, w and $n \equiv c$, o. The dimensionless forms of the governing equations are written as:

$$\frac{\partial c_{fo}}{\partial \tau} + \frac{\partial c_{fo}}{\partial \xi} = -\beta_1[c_{fo} - c_{wo}] \tag{1}$$

$$\frac{\partial c_{fc}}{\partial \tau} + \frac{\partial c_{fc}}{\partial \xi} = -\beta_1[c_{fc} - c_{wc}] \tag{2}$$

$$\frac{\partial \theta_f}{\partial \tau} + \frac{\partial \theta_f}{\partial \xi} = -\beta_2[\theta_f - \theta_w] \tag{3}$$

$$\frac{\partial \theta_w}{\partial \tau} - \frac{1}{Pe_w}\frac{\partial^2 \theta_w}{\partial \xi^2} = \beta_5[\theta_f - \theta_w] + \frac{\beta_3 \beta_5 Da_2 c_{wo} c_{wc} e^{\frac{\gamma\theta_w}{1+\theta_w}}}{(1+\kappa_1 c_{wc})^2} - \beta_4 q_R \tag{4}$$

$$c_{fo} - c_{wo} = \frac{Da_2}{2}\frac{c_{wo} c_{wc} e^{\frac{\gamma\theta_w}{1+\theta_w}}}{(1+\kappa_1 c_{wc})^2} \tag{5}$$

$$c_{fc} - c_{wc} = Da_1 \frac{c_{wo} c_{wc} e^{\frac{\gamma\theta_w}{1+\theta_w}}}{(1+\kappa_1 c_{wc})^2}. \tag{6}$$

The first two equations describe the oxygen and carbon monoxide balances in the gas phase. The energy balances in the gas and solid phases are given by Eqs. 3–4. The last two equations describe the equilibrium between mass transfer to

Current address of N. F. J. van Rensburg: Dept. of Mathematics, Univ. of Pretoria, South Africa.

the surface and the reaction rate. The contribution of radiation to the energy transfer is given by the net radiative heat flux governed by the radiative transfer equation (cf. Min and Shin, 1991):

$$\frac{d^2q_R}{d\xi^2} - 4\epsilon\alpha q_R = \epsilon\frac{d^2(1+\theta_w)^4}{d\xi^2}. \tag{7}$$

The system is closed by the following set of initial and boundary conditions:

$$c_{foi} = 1 \tag{8}$$

$$c_{fci} = 1 \tag{9}$$

$$\theta_{fi} = 0 \tag{10}$$

$$\frac{d\theta_w}{d\xi} = 0, \quad \xi = 0, 1 \tag{11,12}$$

$$\frac{dq_R}{d\xi} - 2\alpha q_R = \epsilon\left[\frac{d(1+\theta_w)^4}{d\xi} - 2\alpha\left((1+\theta_w)^4 - 1\right)\right], \quad \xi = 0 \tag{13}$$

$$\frac{dq_R}{d\xi} + 2\alpha q_R = \epsilon\left[\frac{d(1+\theta_w)^4}{d\xi} + 2\alpha\left((1+\theta_w)^4 - 1\right)\right], \quad \xi = 1. \tag{14}$$

Wendland (1980) demonstrated the importance of enhanced heat- and mass-transfer coefficients at the inlet in a series of experiments. The experimental results of Wendland led us to believe that the inlet effect diminishes more slowly than indicated by the theoretical results of Kay (cf. Knudsen and Katz, 1958). Correlating the data of Wendland, one obtains:

$$Nu = 3.66\left[1 + \frac{0.05226}{\frac{\xi\alpha}{Pe_f} + 0.0166}\right]. \tag{15}$$

The mass-transfer coefficient was evaluated from the following relation, proposed by Votruba et al. (1975):

$$Sh = 0.705\left[Re\frac{D}{L}\right]^{0.43} Sc^{0.56}. \tag{16}$$

Thermo-elastic model

Considering either honeycomb or square channels, it is clear that the most basic element of symmetry of the solid structure which can be identified is a single wall. The dimensions of this element are $L \times H \times \Delta t$, measured in a Cartesian system $x \times y \times z$. Although the system can freely expand in the x-direction, it is restrained in the y-direction. Therefore, the displacement vector (u, v, w) can be written as $(u, 0, 0)$, where u is given by:

$$(\lambda + 2\mu)\frac{d^2u}{dx^2} - (3\lambda + 2\mu)\alpha_T\frac{dT_w}{dx} = 0, \tag{17}$$

where λ and μ are the Lame constants. The axial strain is related to u in the way $\epsilon_{xx} = du/dx$. The stress relations are:

$$\sigma_{xx} = (\lambda + 2\mu)\epsilon_{xx} - (3\lambda + 2\mu)\alpha_T[T_{fi}(1 + \theta_w(\xi)) - T_{\text{ref}}] \tag{18}$$

$$\sigma_{yy} = \lambda\epsilon_{xx} - (3\lambda + 2\mu)\alpha_T[T_{fi}(1 + \theta_w(\xi)) - T_{\text{ref}}] \tag{19}$$

$$\sigma_{zz} = \lambda\epsilon_{xx} - (3\lambda + 2\mu)\alpha_T[T_{fi}(1 + \theta_w(\xi)) - T_{\text{ref}}]. \tag{20}$$

Since $\sigma_{xx} = 0$, one can substitute ϵ_{xx} from Eq. 18 into 19–20 to solve for σ_{yy} and σ_{zz}. We are interested in the compressive stress:

$$\sigma_{yy} = -E\alpha_T[T_{fi}(1 + \theta_w) - T_{\text{ref}}]. \tag{21}$$

All the shear stresses are zero. The introduction of a second reference temperature T_{ref}, where the system is stress free, is necessary to distinguish it from the reference temperature for the chemical reaction model.

The channel wall is loaded along the edges as shown in Figure 1. This load is distributed, since it depends directly on the axial wall temperature and it sets the problem apart from classical plate buckling problems which are usually loaded uniformly. According to von Karman plate theory, the problem of wall deformation can be written as:

$$D_p\nabla^4(\omega) = \sigma_{yy}\Delta t\frac{\partial^2\omega}{\partial y^2} \tag{22}$$

where D_p is the plate flexural rigidity. Inertia is not included in this model, since the loading (σ_{yy}) varies on a time scale associated with heat dissipation, which is several orders of magnitude slower than the time scale for the propagation of mechanical perturbations. Equation 22 describes displacements $\omega(x, y)$ outside the $x - y$ plane. It is a generalized eigenvalue problem of the form:

$$A \cdot \omega = \Lambda B \cdot \omega \tag{23}$$

The spectrum of problem 22 is positive real. If at least one element of the spectrum lies in the interval (0, 1) failure occurs. We can make this formal connection between failure and instability for ceramic monoliths; for metallic structures (which are more ductile) instability and failure are not necessarily associated with the same load.

The boundary conditions which are used for this problem also require some discussion. The edges at $x = 0, L$ are free, while the edges at $y = 0, H$ are fixed. Free edges are described by the following boundary conditions:

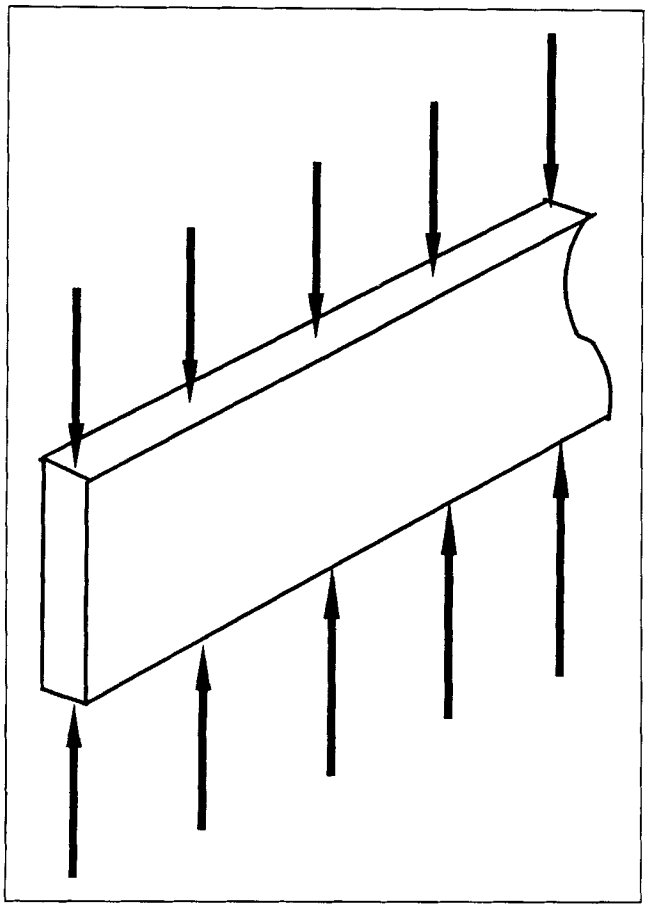

Figure 1. Wall with loading.

$$\frac{\partial^2 \omega}{\partial x^2} + \nu \frac{\partial^2 \omega}{\partial y^2} = 0 \tag{24}$$

$$\frac{\partial^3 \omega}{\partial x^3} + (2 - \nu) \frac{\partial^3 \omega}{\partial y^2 x} = 0. \tag{25}$$

When the edges are clamped, vanishing displacement and vanishing normal slope exist:

$$\omega = 0 \tag{26}$$

$$\frac{\partial \omega}{\partial y} = 0. \tag{27}$$

Results

The set of dimensionless Eqs. 1–4 were discretized using finite differences. This initial value problem was solved, using explicit integration with adjustable time steps. Equations 22 and 24–27 were discretized and the temperature profile $\theta_w(\xi)$ was substituted into Eq. 22 to obtain the form given by Eq. 23. An IMSL subroutine was used to solve the eigenvalue problem.

Thiart (1990) fitted values for ν and α_T as functions of temperature for alumina-based supports:

Table 1. Parameter Values

Item	Units	Value/Expression
ν_f	m^2/s	$(-37.45+0.157_{fi})\times 10^{-6}$
ρ_f	kg/m^3	$342.0/T_{fi}$
$\rho_f Cp_f$	$J/m^3 \cdot K$	$0.014/\nu_f$
ρ_w	kg/m^3	2,500
Cp_w	$J/kg \cdot K$	1,225.0
C_{tot}	mol/m^3	$12{,}214.29/T_{fi}$
C_{fei}	mol/m^3	$0.02 \times C_{tot}$
C_{foi}	mol/m^3	$0.04 \times C_{tot}$
k_o	$m^4/mol \cdot s$	$4.14 \times 10^{11}/C_{tot}^2$
E/R	K	12,600
L	m	0.1016
T_{fi}	K	600
T_{ref}	K	300
$-\Delta H$	J/mol	2.8×10^5
D_f	m^2/s	$\nu_f/0.72$
ϵ		0.4
k_f	$W/m \cdot K$	0.05
k_w	$W/m \cdot K$	27.0

$$\nu = 0.308 - 1.259 \times 10^{-4} t + 2.321 \times 10^{-7} t^2$$

$$\alpha_T = [4.312 + 0.01756t - 2.964 \times 10^{-5} t^2 - 1.843 \times 10^{-8} t^3] \times 10^{-6}$$

where t denotes the temperature in Celsius. These relationships are valid between 0°C and 1,000°C. The parameters of the chemical reaction system are listed in Table 1.

Conditions can vary considerably during startup, changes occur in the air/fuel ratio and gas temperatures at the inlet of the monolith. Oh et al. (1993) found good agreement between experimental and numerical studies of catalytic monoliths for the Federal Test Procedure driving schedule. They used the same kinetic model for CO oxidation as we did, but they did not consider temperature transients in the gas phase and radiation. To demonstrate the application of our criterion during startup conditions, we will keep the inlet gas concentrations for CO and O_2 at 2 and 4%, respectively (with N_2 as balance). The inlet gas temperature is fixed at 600 K. We have decided on this inlet temperature for two reasons: (a) lower inlet gas temperatures have considerably longer times to light-off and (b) the possibility of failure is higher at increased inlet temperatures. However, the criterion can be applied to the Federal Test Procedure protocol in the same way.

In Figure 2 the wall temperature is shown during startup. Initially, the temperature increases faster near the inlet, developing a local maximum. At a later stage the maximum moves towards the outlet until it is established there when a steady state is reached. A simple way to follow the effect of loading on the wall during startup is to plot the smallest eigenvalue as a function of time, as shown in Figure 3. The dimensions of the channel ($L \times H \times \Delta t$) are $101.6 \times 1.04 \times 0.127$ mm. Since the loading is proportional to the temperature profile, the minimum eigenvalue is found when the temperature reaches steady state. In this example, the eigenvalue did not become critical and the monolith can withstand the operating conditions. This evaluation becomes quite important when a monolith is considered for a new application such as burner support, where it will operate beyond existing limits. If the same monolith support will be used in the role of a

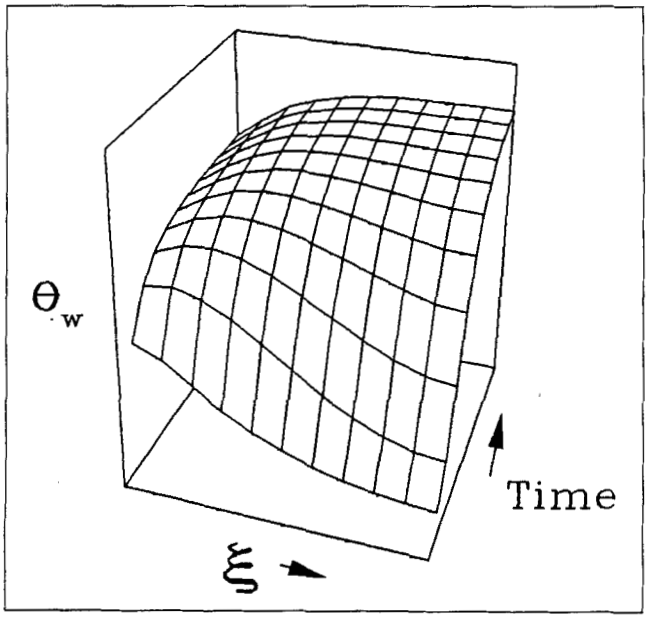

Figure 2. Wall temperature development from startup.

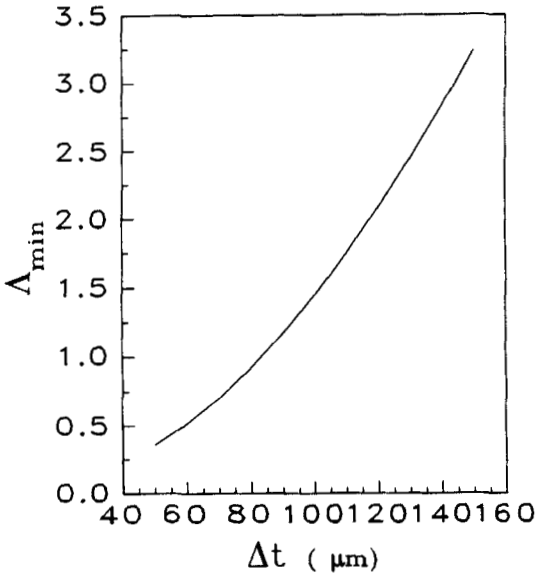

Figure 4. Minimum eigenvalue vs. wall thickness.

porous burner, the temperature will be much higher and the margin for structural soundness will decrease. It is customary to report the strength of ceramic structures under tensile loading in terms of their Weibull parameters and a similar result can be expected in our problem. Some samples will fail before the minimum eigenvalue reaches one; others will withstand loads beyond this point. Turning towards design considerations, we will choose the steady state of Figure 2 as our loading temperature and examine the effects of different wall thicknesses and heights on the minimum eigenvalue. In Figure 4 the minimum eigenvalue is shown as a function of wall thickness. Failure is expected when the wall thickness is less than 0.085 mm. The stability increases with increased wall thickness, and thicker walls seem like a logical solution to the stability problem. However, thicker walls lead to an increase in thermal capacity and the time to light-off is extended. From a thermal point of view one will actually prefer to make the walls as thin as possible. In Figure 5 the effect of wall height is illustrated. As expected, the stability drops off sharply when the slenderness ratio (height:thickness) increases; furthermore overall conversion is not favored by larger channels. Within the limits of reasonable pressure drop, smaller channels are preferable from both mechanical and performance standpoints.

The failure criterion, described by the eigenvalue problem 22 is based on a linear theory, and it is known that it cannot be used for ductile materials, since snap-through can occur at

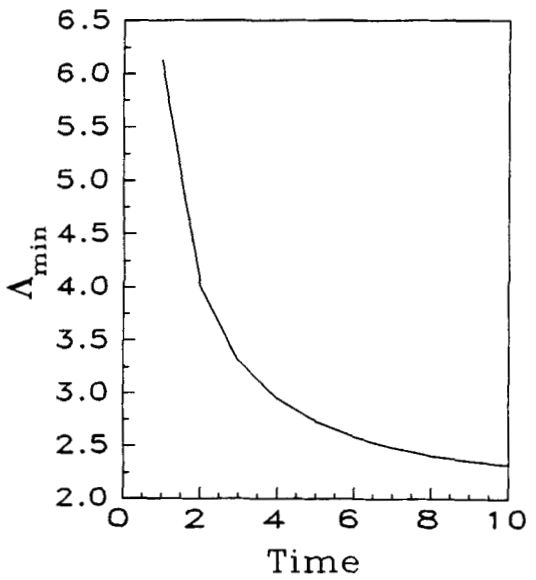

Figure 3. Minimum eigenvalue during startup.

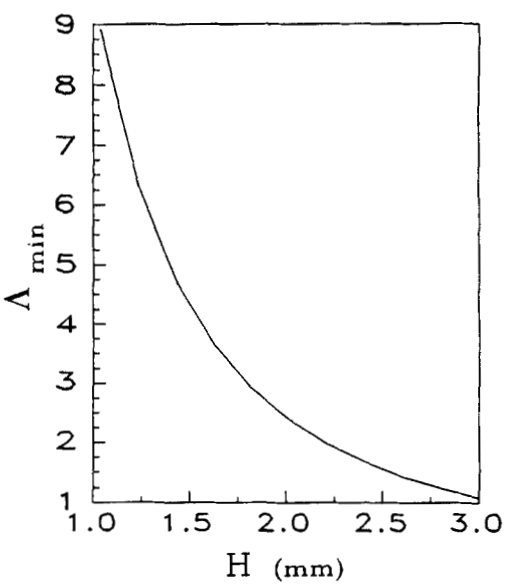

Figure 5. Minimum eigenvalue vs. wall height.

lower loads than the bifurcation value (similar to subcritical bifurcation). For ceramic structures these considerations are obviously not relevant, but a statistical scattering in strength occurs in ceramic materials. Therefore, it is appropriate to define strength in terms of the Weibull parameters. A subcritical load, where $\Lambda_{min} > 1$, is therefore not a sufficient condition that failure will not occur.

There are some additional factors which may affect the mechanical integrity of the monolith. Moisture usually present in the cold monolith and steam entrapment, as well as the leaching of silica from the ceramic structure (cf. Sadler and Davies), can damage the monolith. Thermal shock is potentially present during startup, but it only plays a significant role when the ignition occurs on a time scale that is comparable to acoustic wave propagation in the solid phase.

Acknowledgment

HJV gratefully acknowledges the National Science Foundation for financial support of this work under grant no. CTS-9308813.

Notation

c = dimensionless concentration
C = concentration
Cp = specific heat
D = equivalent channel diameter
$D_p = E_y \Delta t^3/12[1-\nu^2]$
$Da_1 = (k_0 C_{foi})/k_c$
$Da_2 = (k_0 C_{fci})/k_c$
D_f = diffusion coefficient
E = activation energy
E_y = Young's modulus
$(-\Delta H)$ = heat of reaction
k_c = mass-transfer coefficient
k_H = heat-transfer coefficient
$k_{f,w}$ = thermal conductivity
k_0 = frequency factor
k_1 = rate constant
Nu = Nusselt number $k_H D/k_f$
$Pe_{f,w}$ = Peclet number $UL/\kappa_{f,w}$
q_R = dimensionless radiation flux $Q_R/(\sigma_B T_{fi}^4)$
Q_R = radiation flux
R = universal gas constant
Re = Reynolds number $\rho_f DU/\mu_f$
Sc = Schmidt number $\mu_f/\rho_f D_f$
$S_f = \pi D^2/4$
Sh = Sherwood number $\kappa_c D/D_f$
t = time
T = temperature
(u, v, w) = displacement vector
x = axial distance

Greek letters

α = aspect ratio L/D
α_T = thermal expansion coefficient
$\beta_1 = \sigma k_c L/S_f U$
$\beta_2 = (\sigma k_H L)/(S_f \rho_f Cp_f U)$
$\beta_3 = [(-\Delta H) C_{foi} k_c]/k_H T_{fi}$
$\beta_4 = [\sigma_B T_{fi}^4 L]/[\rho_w Cp_w U \Delta t]$
$\beta_5 = k_H L/[U \rho_w Cp_w \Delta t]$
$\gamma = E/RT_{fi}$
ϵ = emissivity
θ = dimensionless temperature
$\kappa_1 = k_1 C_{fci}$
$\lambda = E_y/[2(1+\nu)]$
$\mu = \nu E_y/[(1+\nu)(1-2\nu)]$
μ_f = dynamic viscosity
ν = Poisson ratio
ν_f = kinematic viscosity
ξ = dimensionless spatial variable x/L
ρ = density
$\sigma = \pi D$
σ_B = Stefan-Boltzmann constant
τ = dimensionless time tU/L
ω = displacement out of $x \times y$ plane

Subscripts

c = CO species
f = gas phase
i = inlet condition
o = O_2 species
w = solid phase

Literature Cited

Knudsen, J. G., and D. L. Katz, *Fluid Dynamics and Heat Transfer*, McGraw-Hill, New York (1958).

Min, D. K., and H. D. Shin, "Laminar Premixed Flame Stabilized Inside a Honeycomb Ceramic," *Int. J. Heat Mass Transf.*, **34**, 341 (1991).

Oh, S. H., E. J. Bissett, and P. A. Battiston, "Mathematical Modeling of Electrically Heated Monolith Converters: Model Formulation, Numerical Methods and Experimental Verification," *Ind. Eng. Chem. Res.*, **32**, 1560 (1993).

Sadler, L. Y., and E. G. Davies, "Steam-Induced Volatilization of Silica from Refractories," Report of US Bureau of Mines, 9052 (1986).

Thiart, J. J., "Thermal Stresses in Ceramics," PhD thesis, Univ. of Stellenbosch, South Africa (1990).

Thiart, J. J., et al., "Development of Thermal Stresses in Reacting Media I: Failure of Catalyst Particle," *Chem. Eng. Sci.*, **46**(1), 351 (1991).

Thiart, J. J., S. M. Bradshaw, H. J. Viljoen, and V. Hlavacek, "Thermochemical Stress Development in Ceramic Catalyst Supports," *Chem. Eng. Sci.*, **48**(11), 1925 (1993).

Votruba, J., O. Mikus, K. Nguen, V. Hlavacek, and J. Skrivanek, "Heat and Mass Transfer in Monolithic Honeycomb Catalysts: II," *Chem. Eng. Sci.*, **30**, 201 (1975).

Wendland, D. W., "The Segmented Oxidizing Monolith Catalytic Converter," *Trans. ASME*, **102**, 194 (1980).

Manuscript received May 2, 1994, and revision received July 28, 1994.